

# Requirements for and development of 2 dimensional X-ray detectors for the European X-ray Free Electron Laser in Hamburg

---

**Heinz Graafsma**

*DESY and European XFEL  
Notkestrasse 85, 22607 Hamburg, Germany*

*E-mail: [heinz.graafsma@desy.de](mailto:heinz.graafsma@desy.de)*

**ABSTRACT:** The source characteristics of the European XFEL and the planned experimental facilities that are relevant for the X-ray detectors are presented, and the requirements for the 2-dimensional X-ray Detectors are stated and explained. It is clear that, although these requirements will evolve with time, they demand new detector concepts to be developed. Three X-ray detector development projects have been initiated by the European XFEL, each using a conceptually different approach to meet the stringent requirements. The basic principles used in the projects are briefly presented.

**KEYWORDS:** X-ray detectors; Instrumentation for FEL; Solid state detectors

---

## Contents

<b>1</b>	<b>Introduction</b>	<b>1</b>
<b>2</b>	<b>Source parameters and scientific applications at the European XFEL</b>	<b>2</b>
2.1	The Radiators	3
<b>3</b>	<b>Requirements for the 2-dimensional X-ray detectors</b>	<b>4</b>
3.1	Generic consequences for the X-ray detectors	4
3.1.1	Photon energy range	4
3.1.2	Single shot imaging	5
3.1.3	Frame storage	5
3.1.4	Central hole	6
3.1.5	Radiation tolerance	7
3.2	Application specific consequences for the X-ray detectors	7
3.2.1	Angular coverage or size of the detector	7
3.2.2	Angular resolution, pixel size and number of pixels	9
3.2.3	Sample to detector distance	10
<b>4</b>	<b>2D Detector Projects for the European XFEL</b>	<b>11</b>
4.1	The Adaptive Gain Integrating Pixel Detector (AGIPD) project	11
4.2	The Large Pixel Detector (LPD) project	12
4.3	The DEPFET Sensor with Signal Compression (DSSC) project	13
<b>5</b>	<b>Summary</b>	<b>14</b>

---

## 1 Introduction

The European X-ray Free-Electron Laser Facility is a new international scientific infrastructure under construction in the north-west of Hamburg, that will be entering user operation in 2014. The purpose of the Facility is to generate extremely brilliant (peak brilliance  $\sim 10^{33}$  photons/s/mm<sup>2</sup>/mrad<sup>2</sup>/0.1%BW), ultra-short (< 100 fs) pulses of spatially coherent X-rays with wavelengths down to 0.1 nm, and to exploit them for revolutionary scientific experiments in a variety of disciplines spanning physics, chemistry, materials science and biology [1]. The basic process adopted to generate the X-ray pulses is SASE (Self-Amplified Spontaneous Emission) [2, 3], whereby electron bunches are generated in a high-brightness gun, brought to high energy (up to 17.5 GeV) through a superconducting linear accelerator, and conveyed to long (up to  $\sim 200$  m) undulators where the X-rays are generated. In the so-called start-up scenario three photon beamlines (SASE-1, SASE-2 and SASE-3) will deliver photons to 6 experimental stations. In the final layout, five photon

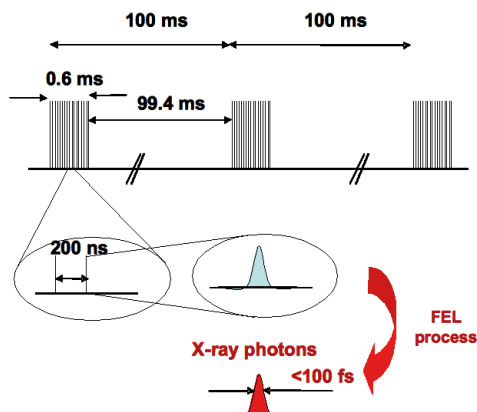


**Figure 1.** Time structure of the European XFEL source; electron bunch trains, with up to 3000 bunches in  $600 \mu\text{sec}$ , repeated 10 times per second. Producing up to 30 000 X-ray pulses per second of less than 100 fsec.

beamlines deliver the X-ray pulses to ten experimental stations. The site and layout even allows for the possibility of a second photon branch extending the number of photon beamlines to 10.

The photon pulse length will be approximately 1000 times shorter than at classical 3<sup>rd</sup> generation Synchrotron storage rings, the horizontal emittance a factor of 100, and the vertical emittance a factor of 3 smaller, the number of photons per pulse a factor of 300 higher, and the natural monochromaticity a factor of 10 better, giving an increase in peak brilliance of 9 orders of magnitude. Another major difference is the fact that at the European XFEL the beam will be fully laterally coherent. It is evident that these improvements will allow for new science to be performed [1] and will revolutionize the way experiments are performed; with the consequence that new type of X-ray detectors will be required.

In this manuscript we will start with a presentation of the source parameters and planned scientific applications of the European XFEL. In the second part, first the generic and application independent consequences for the 2-dimensional X-ray detectors will be given, followed by the application specific detector requirements. In the final section three detector development projects financed by the European XFEL project will shortly be presented.

## 2 Source parameters and scientific applications at the European XFEL

Many of the requirements and challenges described in the rest of this manuscript are intrinsic and common to all X-ray Free Electron Laser sources, irrespective of their time structure. However, an additional challenge for the detectors at the European XFEL, as compared to others like the Linear Coherent Light Source (LCLS) in the USA, the SPring-8 Compact SASE Source (SCSS) in Japan or the FERMI project in Italy, is the non-uniform time structure of the source. LCLS and SCSS use so called “warm” (meaning non-superconducting) accelerator technology and produce 120 and 60 evenly spaced pulses per second, respectively. The European XFEL uses superconducting accelerating cavities, originally developed for the linear collider TESLA, with the advantage of being able to produce up to 30 000 pulses per second. However these pulses are delivered in bunch trains, 0.6 msec long, containing 3000 bunches, followed by 99.4 msec gaps as is depicted in figure 1.

**Table 1.** Properties of the 5 radiators foreseen in the baseline design, extracted from table 5.2.2 and 5.3.2 of the TDR.

	SASE-1	SASE-2	SASE-3	U-1 / U-2
Length [m]	201.3	256.2	128.1	61
Energy [keV]	12.4	3.1–12.4	0.25–3.1	20–90
Photons/pulse	$10^{12}$	$1.6 \times 10^{13} - 10^{12}$	$3.7 \times 10^{14} - 1.6 \times 10^{13}$	$1.1 \cdot 10^9 - 1.9 \cdot 10^9$
Beam size ( $\mu\text{m}$ )	70	55–85	90–60	24.5
Beam div. ( $\mu\text{rad}$ )	1	3.4–0.84	18–3.4	3.0–2.0
Spectral BW (%)	0.08	0.18–0.08	0.65–0.2	0.77–2.33

In other words, all the pulses are delivered in 0.6% of the time, which has major consequences for the experimental conditions and specifically for the 2-dimensional X-ray detectors as will be described in the following sections.

## 2.1 The Radiators

In the base line design, as described in the Technical Design Report (TDR) [1], 5 radiators (undulators) will deliver X-ray photons to 10 experimental stations. It is important to point out at this stage that the TDR provides rather a reference frame, and the exact configuration of the final facility is constantly developing and being adjusted following the rapidly evolving scientific application fields. The properties of the 5 radiators as defined in the TDR are given in table 1 below.

The 10 experimental stations will serve each different fields of science. The TDR identifies the following 8 fields:

1. Small Quantum Systems (SQS)
2. High Energy Density Matter (HED)
3. Coherent X-ray Scattering and Lensless Imaging in Materials Science (CXI)
4. X-ray Photon Correlation Spectroscopy (XPCS)
5. X-ray Absorption Spectroscopy (XAS)
6. Femtosecond Diffraction Experiments (FDE)
7. Single Particles and Biomolecules (SPB)
8. Research And Development (RAD)

A detailed description of the science and experimental requirements for these 8 areas, can be found in the TDR. In the so-called start-up phase, with reduced budget, only the three SASE stations will be built, with SASE-3 limited to linear polarization. This start-up scenario allows for future extension to the full facility described in the TDR. Each of the SASE radiators will

**Table 2.** Experimental stations and assigned scientific applications.

SASE-1	Station 1	Single Particles and Biomolecules (SPB)
	Station 2	Coherent X-ray Scattering and Lensless Imaging in Materials Science (CXI) and X-ray Photon Correlation Spectroscopy (XPCS) in the hard X-ray regime
SASE-2	Station 3	Femtosecond Diffraction Experiments (FDE)
	Station 4	High Energy Density Matter (HED)
SASE-3	Station 5	Small Quantum Systems (SQS)
	Station 6	Coherent X-ray Scattering and Lensless Imaging in Materials Science (CXI) and X-ray Photon Correlation Spectroscopy (XPCS) in the soft X-ray regime

provide the photon beam to 2 experimental stations, and table 2 shows the current planning of the experiments approved for the start-up phase.

Whereas, SQS, HED, XAS and RAD do not require specific large size 2-Dimensional X-ray detectors as their main detecting unit, the other fields CXI, XPCS, FDE and SPB critically depend on it. In the following we will describe both the general and specific requirements for the X-ray detectors at the European XFEL.

### 3 Requirements for the 2-dimensional X-ray detectors

In the first part of this section we will present the general and application independent detector requirements. The second part then deals with the application specific requirements.

#### 3.1 Generic consequences for the X-ray detectors

##### 3.1.1 Photon energy range

The specific source parameters of the European XFEL, as well as the planned experiments, described above, have some general implications for the X-ray detectors. First of all the very large energy range from 250 eV for SASE-3 up to 90 keV for U1 and U2 can not be covered by a single detector or detector technology. Even when only focussing on the three SASE stations the energy range is still too large to be covered by a single optimized detector. This means that different systems need to be developed, each one optimized for a limited energy range, rather than developing one detector per scientific application. For example, as indicated in table 2, CXI and XPCS experiments are planned for both SASE-1 (station 2) and SASE-3 (station 6), and although many detector requirements are the same for use at both stations, the photon energy range is so different that either different detectors, or at least different optimizations will be needed. The detectors used at the lower energy range at SASE-3 will have to be in the same vacuum as the experiments (windowless beamline), and thus have to be vacuum compatible. In the case silicon is used as the detecting element (direct detection), as is the case for the detector development projects described further on, even the entrance surface on the detector has to be specially fabricated in order to reduce the photon

absorption by the insensitive surface layers. For the detectors for the harder X-rays at SASE-1, the situation is simpler, since they can be used outside the sample chamber using X-ray transparent, but optically opaque windows. Also the surface passivation of sensors is much less critical. Another difference is the signal generated per absorbed photon. If direct detection in silicon is used, a 0.25 keV photons will only generate  $250/3.62 = 70$  electron hole pairs, thus in order to be able to detect single photons, a detection and amplification with a noise performance well below 25 electrons is needed (for a minimum  $3\sigma$  separation between signal and noise), at the same time it is desired to be able to measure up to  $10^3$  or  $10^4$  photons per pulse per pixel. If this same system is used at 12 keV generating 3315 electron-hole pairs per absorbed photon, the useable dynamic range is reduce by a factor of 50, making single photon sensitivity at 0.25 keV and a large dynamic range at 12 keV incompatible. Thus not only the silicon sensor, but also the signal processing electronics will need to be differently optimized for the different photon energies.

The different photon energies will also have a very different consequence for possible radiation damage, in particular for underlying microelectronics in case of hybrid pixel detectors. Whereas 0.25 keV is fully absorbed by 300 micron thick silicon sensors, 25% of the 12 keV photons will be transmitted, in which case special radiation hard electronic structures need to be used, that are more space consuming than regular structures, thus reducing the functionality per unit area. Again a separate optimization for the different photon energy ranges seems appropriate.

### 3.1.2 Single shot imaging

The very high peak brilliance, will not only allow for, but in many cases even impose single shot experiments. For instance, the focussed beam will have such a high photon density that the sample under study will not survive a single shot [4, 5], this means that every single shot will have to be treated as a separate experiment, and the complete X-ray scattering image has to be recorded in a single 100 fsec pulse. For the image to be of statistical relevance many pixels will have to record more than one photon. This excludes photon counting, which is normally used to achieve excellent signal to noise ratios [6–8]. Consequently for single shot experiments integrating X-ray detectors will have to be used. At the same time, many of the imaging and XPCS experiments require single photon sensitivity, especially in the high angle regions. It is to be pointed out that there might nevertheless be certain experiments, where the sample is static and not, or only negligibly, damaged by the beam, in which cases multiple images can be summed together in the detector, as is customary at storage ring sources. Even photon counting could be used, provided the scattered intensity is not too high, so that either never more than one photon is absorbed per pixel, or pulse pile-up corrections can be used. In these cases one could still take advantage of the short pulse duration, via a short delay between pump and probe for instance, or from the full lateral coherence of the beam. It is worth pointing out at this point that current storage rings are also pulsed sources, with about 100 pico-second pulse lengths, equally excluding counting more than one photon per pulse. Photon counting 2D X-ray detectors can, nevertheless, frequently be used due to the low scattered photon flux, and the fact that the sample is not destroyed in a single pulse.

### 3.1.3 Frame storage

Figure 1 showed the specific time structure of the European XFEL, with up to 3000 X-ray pulses, separated by 200 nsec, per pulse train and 10 pulse trains per second. Since the large number of

pulses per second is one of the main differences between the European XFEL and the other FEL sources under construction in Europe, the USA and Japan, it is evident that the X-ray detectors should allow taking advantage of this high repetition rate. Consequently, for single shot imaging, a complete image has to be recorded every 200 nsec (5 MHz) during 0.6 msec. Since with current technology it is still impossible to transmit a full image in 200 nsec, the recorded images will have to be stored inside the front-end of the detector, and read out during the inter train period of 99.4 msec. This means either an analogue or digital pipeline per pixel. Ideally, the detector should be able to store 3000 images during the pulse trains, which would mean large pixel sizes, which is not acceptable for many applications. Therefore a compromise, based on the scientific application, is most likely needed between maximizing the number of images that can be stored inside a pixel, and minimizing the size of the pixel. It is worth to point out at this point that each electron branch can only handle half of the total number of electron bunches over an extended time, due to limitations of the electron beam dumps. In case an analogue pipeline is used, one has to assure that the signal droop due to the leakage of both the storage capacitors and the switches does not degrade the accuracy, meaning that droop induced errors have to be much smaller than the photon Poisson statistical uncertainty. For digital pipelines this is not an issue of course.

Fast triggering, and vetoing should be possible so only useful images are recorded and stored, this can be useful for instance when fast moving samples are used, and not every X-ray pulse overlaps with the sample in time and space, or after a successful “hit” some time is needed for the remnants of the sample to be removed, and subsequent pulses should be vetoed. Since the machine is based on the SASE principle, where the amplification process starts from random noise fluctuations, the accelerator might occasionally produce low intensity and unusable pulses. Since the machine has great flexibility in the filling pattern of the bunch train, the detector should be programmable to receive any bunch pattern. This is also important for testing and using the detectors at other X-ray sources.

### 3.1.4 Central hole

Since the focussed primary X-ray beam has sufficient energy to ablate most materials, small primary beam stops can not be used in front of the detectors, as is customary at storage ring sources. Therefore, the X-ray imaging detectors in the forward scattering direction need to have a central hole to let the direct beam through. In order to minimize the loss of small-angle data, which are crucially important in image reconstructions for instance, this hole has to be as small as possible, while still being large enough to allow for occasional small fluctuations in the direct beam position. An attractive alternative is to use one detector close to the sample, covering the weaker wide-angle scattering signals, and having a relatively large hole to let the intense small-angle signal plus the direct beam through. A second detector is then placed at a larger distance covering the small angle scattering part [9]. This has the advantage that the hole size in the first detector becomes less critical. Furthermore, the dynamic range per detector is then reduced, the close by detector covering the weaker signals, and the far away detector the stronger signals. Due to the larger distance, the angular coverage and thus the total intensity per pixel will also be reduced.

### 3.1.5 Radiation tolerance

Another issue of major concern is the radiation tolerance of the detectors, especially when used at the harder X-ray energies of 12 keV. Some of the experiments expect a maximum of  $5 \cdot 10^4$  photons per pulse per pixel of  $200 \mu\text{m} \times 200 \mu\text{m}$  and for small angle scattering, as well as for liquid scattering experiments, for example, these intense parts will always be more or less in the same place on the detector. If we assume that the facility will operate for 5000 hours per year, and every beamline has two experimental stations equally sharing the beamtime, if we further estimate that an experiment takes real data for at most 50% of the time (the other 50% is needed for setup and alignment) we can estimate that the detector will take data for 1250 hours per year. Since each branch of the photon beam systems cannot take more than 15000 pulses per second on average, due to limitations of the electron beam dump system, we get a total of  $6.75 \cdot 10^{10}$  pulses per year. This amounts to a total of  $3.4 \cdot 10^{15}$  photons for the hottest pixels per year, or  $10^{16}$  photons integrated over 3 years. For 12 keV photons and a 500 micron thick silicon sensor, this corresponds to a total absorbed dose of 1 Giga Gray. The above calculation shows clearly that this is a worst case scenario, and the total integrated dose might well be much lower. Nevertheless, the detectors should be designed to withstand the maximum possible dose. Again there might be a compromise needed between the pixel area and the radiation tolerance. At this point it might be interesting to point out that although the peak brilliance will be 9 orders of magnitude higher at the European XFEL than at third generation storage rings, the time integrated flux on the sample will be very similar, therefore, one could expect that the total dose on the detector will also be comparable between XFEL and storage ring sources, but this will depend strongly on the type of experiments that will be performed. Therefore, at this point in time, it is nearly impossible to give final numbers on the expected radiation dose.

## 3.2 Application specific consequences for the X-ray detectors

In the previous section we have described the general requirement for the 2D X-ray detectors stemming from the source characteristics. In this section we will discuss the requirements specific to the applications.

### 3.2.1 Angular coverage or size of the detector

The angular coverage of the detector that is needed in the experiments strongly depends on the scientific question that is sought to be answered and the wavelength of the radiation being used. As a general guideline we can, however, state that the reason to build an X-ray FEL producing 12.4 keV (0.1 nm) X-rays, is to be able to investigate structures down to the atomic level (0.1 nm). In the FDE, CDI, and SPB experiments the structures are investigated using X-ray diffraction, and in order to distinguish features of 0.1 nm with 0.1 nm radiation, Bragg's law shows that one has to measure the scattered angle to at least 60 degrees, or in other words a momentum transfer  $Q$ , defined as  $Q = 4\pi \times \sin(\theta)/\lambda$  of  $2\pi \text{ \AA}^{-1}$  is needed. Since in almost all cases one wants to measure both the positive and negative scattering angles, the total coverage should extend 120 degrees. In the case of pump-probe measurements on liquid samples, which are part of the FDE suite of experiments, one has to measure to even larger momentum transfers, in order to be able to scale between the excited and ground state signals. A momentum transfer of  $10 \text{ \AA}^{-1}$  is needed, which corresponds for 0.1 nm



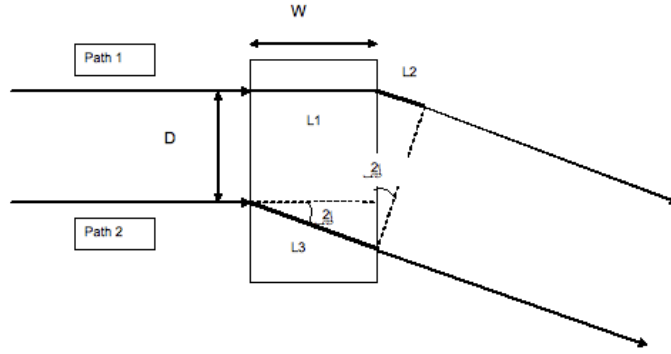


**Figure 2.** Geometrical layout of small angle scattering experiment, the ray on the top is scattered from the backside of the sample with thickness  $W$ , and the bottom ray is scattered from the frontside. The width of the beam is  $D$ .

radiation to a total angular range (positive and negative scattering angle) of 200 degrees. Note that this angular range cannot be covered by a single flat detector, and one either has to use multiple segmented detectors, with the associated challenges to calibrate the segments with respect to each other, or one has to use a higher photon energy, like the third harmonic of one of the SASE radiators or one of the spontaneous radiators U-1 or U-2. For the XPCS experiments two situations can be distinguished: small angle scattering and crystalline diffraction [10]. For small angle scattering, if one would like to study the dynamics at length scales down to 10 nm using 0.1 nm radiation (SASE-1) Braggs law gives a required scattering angle of 0.6 degrees, and thus a required detector span of 1.2 degrees (positive and negative scattering angles). This range will, however, be reduced in those cases where no monochromator is used, due to the limited longitudinal coherence length and path length differences (PLD) in rays hitting one pixel. Figure 2 shows the geometrical layout of a small angle scattering experiment of a sample with thickness  $W$  and a beam size  $D$ . It can be shown that the PLD between ray 1 and ray 2 is given by

$$PLD = 2W \sin^2 \theta + D \sin 2\theta \quad (3.1)$$

In XPCS experiments, as in all coherent scattering experiment, one needs the various rays hitting a pixel to be coherent. Therefore, the PLD has to be smaller than the longitudinal coherence length, which is given by [11]

$$\xi_1 = \frac{\lambda^2}{\Delta\lambda}$$

where  $\lambda$  is the wavelength and  $\Delta\lambda$  the bandwidth or monochromaticity. The natural bandwidth, i.e. without monochromator, of the SASE-1 radiation of 0.1 nm is 0.1% or  $10^{-4}$  nm; giving a longitudinal coherence length of 100 nm. If we now assume a sample thickness  $W$  of 1 mm, and a typical beamsize  $D$  of 25  $\mu\text{m}$  and a maximum allowed PLD equal to the longitudinal coherence length of 100 nm, equation 1 shows that the maximum allowed scattering angle is approximately 0.1 degrees, giving a total detector coverage of 0.2 degrees. It is possible to use a monochromator to decrease the bandwidth and thus increase the longitudinal coherence length, this at the expense of flux, and special care must be taken not to destroy the lateral coherence of the beam. One should note that in small angle scattering experiments the distance between the sample and detector has to

be large in order to get access the long length scales, and can be up to 40 meters in the case of the European XFEL. Thus, although the required angular coverage is small, the linear dimensions of the detector are not.

### 3.2.2 Angular resolution, pixel size and number of pixels

Another parameter that is directly determined by the scientific question under study, and that shows a large dispersion amongst the different application is the angular resolution which is determined by the pixel size and the sample to detector distance. Often application scientists will quote a certain pixel size as a requirement for their experiment, whereas the real requirement is the angular resolution, with the pixel size and the sample to detector distance as somewhat free parameters. Certain other requirements, like in vacuum operation for instance, might impose boundaries for the sample to detector distance and other technological considerations might limit the freedom in the choice of the pixel size. However, in almost all cases, the angular resolution is the real experimental requirement, and the pixel size a resulting detector specification. The required angular resolution is determined by the highest spatial frequency in reciprocal space needed.

For the applications currently foreseen at the European XFEL, the lowest angular frequency is required for the FDE experiments on non-crystalline samples. In these experiments one dissolves the molecule under study into a liquid, and compares the total liquid scattering pattern with and without a pump excitation. Since the total scattering pattern contains contributions from both the dissolved molecules and the solvent and one has to extract small changes against a large background signal, these studies are necessarily limited to changes in a few atomic distances only. One can show [1] that small changes in inter-atomic distance result in approximately 5 oscillations in the Q range between 0 and  $10 \text{ \AA}^{-1}$ , for complete rupture of bonds, and thus dissociation of the molecule one might get up to 10 oscillations for this range. Since the number of inter-atomic distances under study is limited, a total number of 250 sampling points between  $Q=0$  and  $10 \text{ \AA}^{-1}$  is largely sufficient. In order to cover both positive and negative scattering angles 500 pixels are needed. As shown in the section on total angular coverage of  $Q = 10 \text{ \AA}^{-1}$  with 0.1 nm radiation corresponds to 200 degrees scattering angle, giving an angular resolution of  $200/500 = 0.4$  degrees (or 7 mrad). Even for sample to detector distances as small as 10 cm, this would correspond to a comfortably large pixel size of 700 microns.

XPCS is at the other end of the spectrum, with the highest required angular resolution of all applications. In order to get the highest quality time-correlated data, one should have not more than one speckle per pixel, meaning that the pixel size should be equal or smaller than the speckle size. The angular speckle size  $\theta_s$  in turn is given by

$$\theta_s = \frac{\lambda}{D} \quad (3.2)$$

where  $\lambda$  is the wavelength and D the size of the laterally coherent part of the incident beam, which at the XFEL is nearly the full beam. Equation 2 shows that the angular speckle size can be tuned by tuning the width D of the incident beam using focussing elements. The optimum choice will be a trade-off between using a large beam with negligible sample heating or radiation damage, but giving impractically small speckles, and using a focussed beam giving comfortably large speckle sizes but a too high power density on the sample. If we choose a practical incident beam size of

25 microns, and a wavelength of 0.1 nm, we get an angular speckle size of  $4 \mu\text{rad}$ . At a sample to detector distance of 40 meters this would still require pixels not larger than  $160 \mu\text{m}$ .

One possible solution to obtain small effective pixels would be to use an adjustable double grid in front of detector. By adjusting the two grids one can tune the effective pixel size, while keeping the same pitch. In the optimum case, the holes in the grids should be exactly half the pixel size, allowing tuning the effective pixel size down to 0. Since in XPCS experiments the pixels are individual counters, and since the total number of pixels is not affected by using grids, this should have no effect on the statistical accuracy of the measurements, provided there are enough speckles spread out over the entire detector area. The effect of non-continuous sampling of the speckle pattern will need detailed investigation, but the possibility to have variable effective pixel sizes seems attractive enough to investigate this option. Interestingly enough, since the effective pixel size can be made arbitrarily small using the grids, the required real pixel size for XPCS would not be smaller than the smallest speckle, but rather larger than twice the biggest speckle.

For the coherent imaging experiments, CDI and SPB, we have seen that, in order to resolve structural features down to the atomic level of 0.1 nm, we have to measure out to a scattering angle of  $\pm 60$  degrees. If we want to investigate samples up to 100 nm in diameter, for instance large viruses, with 0.1 nm resolution, the Nyquist theorem imposes 2000 sampling points, giving a required angular resolution of 0.03 degrees (or 0.5 mrad). This is expressed by the following equations:

$$\begin{aligned} 2\theta_{\max} &= a \sin\left(\frac{\lambda}{2d_{\min}}\right) \\ N &= 2\frac{D}{d_{\min}} \\ \Delta 2\theta &= \frac{2\theta_{\max}}{N} = \frac{a \sin\left(\frac{\lambda}{2d_{\min}}\right)}{2D} d_{\min} \end{aligned}$$

Where  $2\theta_{\max}$  is the maximum scattering angle required;  $2d_{\min}$  the smallest structural feature desired;  $N$  the number of sampling points and  $D$  the size of the sample. The formulae show that less structural details require less angular coverage and smaller structures less angular resolution.

### 3.2.3 Sample to detector distance

The sample to detector distance is to some degree a free variable, which can be chosen so as to tune the angular coverage and resolution, having a detector with given pixel size and number of pixels. The minimum sample to detector distance will most often be determined by both the sample environment, like sample injectors, cryogenic stages, furnaces, pressure cells, etc. and the minimum angular resolution required. At Storage Ring sources, with comparable sample environments, the sample to detector distance is seldom less than 50 mm, and most often more than 100 mm. But it is clear that this will depend directly on the experiment at hand. The maximum sample to detector distance will be determined by various factors. First of all the size of the experimental hall of the European XFEL will limit the absolute maximum sample to detector distance to approximately 40 meters, the experimental hall being 50 meters deep.

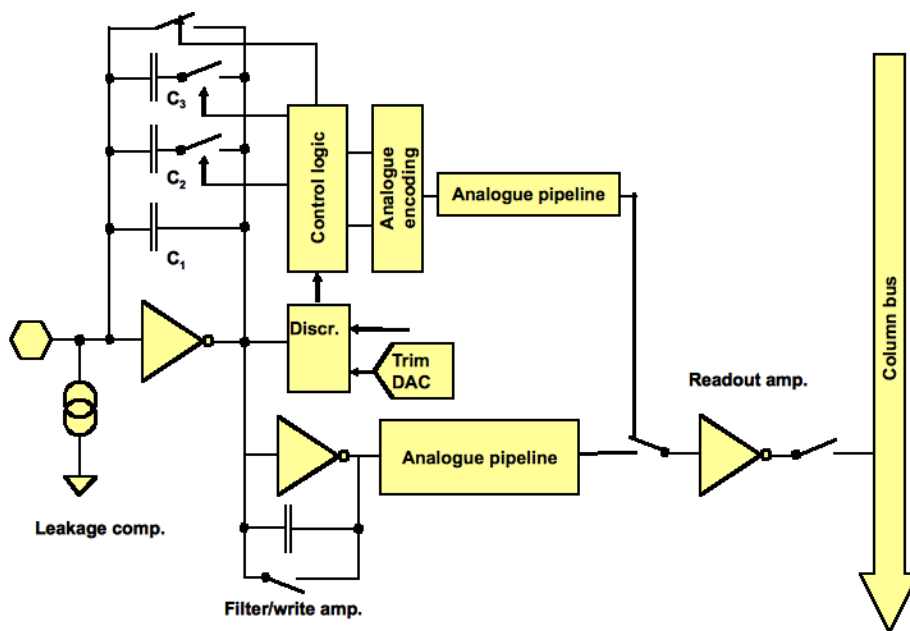


Figure 3. Schematic layout of the pixel cell for the AGIPD detector.

## 4 2D Detector Projects for the European XFEL

In order to meet the challenges indicated above, the European XFEL launched a call for proposals in 2007. As a result of this call the European XFEL is now financing three independent detector development projects that attempt to solve the high burst mode frame rate and the required high dynamic range in different ways, and at the same time target different applications and/or wavelength ranges. The basic principles of the three projects will be described in this section. It is to be pointed out that there are similar projects under way in the USA for the LCLS project [12, 13].

### 4.1 The Adaptive Gain Integrating Pixel Detector (AGIPD) project

The Adaptive Gain Integrating Pixel Detector (AGIPD) is developed by a consortium of DESY (coordinator), PSI/SLS, university of Hamburg and university of Bonn, and consists of a classical hybrid pixel array, with readout ASICs bump-bonded to a silicon sensor. The ASIC is designed in 8 metal layer 0.13  $\mu\text{m}$  CMOS technology and uses dynamic gain switching to cover the large dynamic range, and an analogue pipeline to store recorded images during the 0.6 msec long bunch train, that are subsequently readout and digitized during the 99.4 msec interval between bunch trains. A schematic layout of the pixel cell is given in figure 3 [14].

The first stage is a charge sensitive amplifier, with three different gain settings that are dynamically switched. Special care has to be taken to insure that the charge injected by the gain switching is well below the photon-counting statistical noise [15]. For every image recorded, the corresponding gain setting is stored in a pipeline. In case the global intensity distribution in the image is known beforehand the gain settings can be preset and fixed. After amplification the signal is stored in an analogue pipeline. The storage capacitors in the pipe-line have to be low leakage, which is possible using either MIM (Metal-Insulator-Metal) capacitors or DGN (dual oxide n-FET

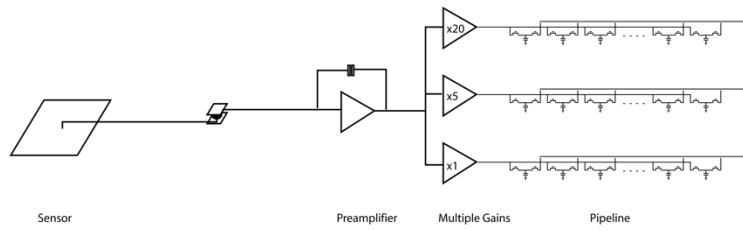


**Figure 4.** Schematic layout of the LPD pixel cell.

in n-well) capacitors. A major concern, however, are the switches, that should permit charging the capacitors within the 200 nsec inter-bunch spacing, but prevent discharging due to leakage during the 100 msec inter-train spacing. With advanced switch designs it is possible to reach this performance criterium, but at the same time the storage cells have to be kept as small as possible in order to record the maximum possible number of images during the bunch train. The design goals are  $200 \mu\text{m} \times 200 \mu\text{m}$  pixels, containing more than 200 storage capacitors, with  $64 \times 64$  pixels per chip.  $2 \times 8$  chips will be bump-bonded to single Si-sensors constituting the basic module building block. The silicon sensors and readout ASICs will be mounted in vacuum, while the interface electronics will be housed at ambient pressure, in order to facilitate access for maintenance. The detector will consist of four quadrants and a central hole for the direct beam. The quadrants can be moved with respect to each other in order to adjust the central hole size. The interface electronics is responsible for the digitization during readout, for providing trigger signals during data taking in order to synchronize to the photon bunches, and for the slow control signals. The communication with the backend is via 10 Gigabit links. The main scientific applications are Coherent X-ray imaging and Photon Correlation Spectroscopy at 12 keV photon energies. A full detector simulation program, HORUS, is written, in order to study the scientific impact of various detector limitations and necessary compromises between conflicting requirements [16, 17].

## 4.2 The Large Pixel Detector (LPD) project

The LPD project attempts to achieve the large dynamic range required, by employing 3 different gain settings in parallel, each followed by its own analogue pipe line. The principle is depicted in figure 4.

To implement 3 analogue pipelines in parallel per pixel with 500 storage cells each, the pixel size amounts to  $500 \mu\text{m}$ , which is relatively large for some photon science applications, and hence its name. The LPD-project is managed by the detector group of the Rutherford Appleton Laboratory and executed in conjunction with the University of Glasgow.

The LPD front-end module will include an interposer between the silicon sensor and the ASIC, which gives the flexibility to have different pixel sizes and layouts between the silicon sensor and the ASIC. It also provides extra radiation shielding, relaxing the required radiation hardness of the ASIC. Each chip will contain  $16 \times 32$  pixels and  $8 \times 1$  chips will be bump-bonded to a monolithic silicon sensor giving  $128 \times 32$  pixels tiles.  $2 \times 8$  of these tiles will be used to construct so called super modules with  $256 \times 256$  pixels. These super modules can then be used to construct detectors of any size, including a central hole for the direct beam transport [18]. An interesting

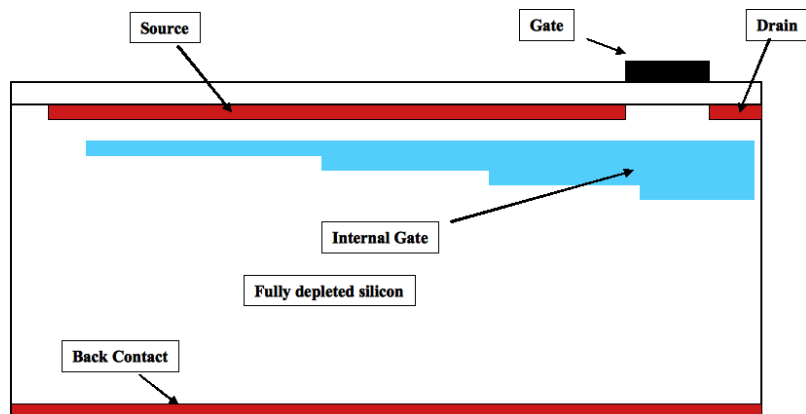


**Figure 5.** Principle of the DEPFET with non-linear signal response.

option for the LPD is to string together the 3 different analogue pipelines, in case the required gain setting is known beforehand, which is normally the case for liquid scattering experiments, where the scattering pattern is very reproducible. This will allow to record up to 1500 images per bunch train, and thus a near optimal use of the high luminosity of the European XFEL. The LPD focuses on the 12 keV photon energy range, and is optimally suited for liquid scattering experiments.

### 4.3 The DEPFET Sensor with Signal Compression (DSSC) project

The DEPFET Sensor with Signal Compression, DSSC, uses a non linear response of the active sensor pixels to cope with the large dynamic range, and a digital memory to store images inside the pixels [19, 20]. The DSSC project is developed by a consortium consisting of the MPI-Semiconductor Lab in Munich (coordinator), the Politecnico di Milano, DESY-Hamburg, and the Universities of Heidelberg, Siegen and Bergamo. The principle of a single DEPFET of the DSSC sensor is given in figure 5.

The electrons generated by absorbed photons are stored in the internal gate underneath the gate of the FET, like in a standard DEPFET [21]. However, in the DSSC DEPFET design, the internal gate extends beyond the gate region into the source region. As a result the first electrons generated will be stored right under the gate, giving a large effect on the source drain current, whereas, subsequent electrons will be stored only partly under the gate and increasingly under the source region, thus having a reduced effect on the source drain current, giving the non-linear gain response. An additional advantage of the DEPFET is the low noise performance, which makes this detector well suited for experiments using lower energy X-rays, down to a few hundred eV. The DSSC design foresees hexagonal pixels, which give a more homogeneous drift field and a faster charge collection than square pixels, and with 136  $\mu\text{m}$  long sides results in a 200  $\mu\text{m}$  bump-bond pitch, the minimum provided by the 0.13  $\mu\text{m}$  IBM CMOS process used for the ASIC design.

The DEPFET sensor will be bump-bonded to readout ASICs with an amplifier, shaper and ADC per pixel as well as digital storage memories. The advantage of digital storage over analogue is the absence of signal leakage. The added challenge, however, is the high speed on chip digitization. The baseline design foresees the possibility to store more than 500 images per bunch train. The readout ASIC will have  $64 \times 64$  pixels, and  $2 \times 4$  ASICs will be bump-bonded to a monolithic

DEPFET sensor. Two of these monolithic units will be used to build a ladder with  $128 \times 512$  pixels, that can then be stitched together to form the final  $1k \times 1k$  detector.

In addition to the three large area X-ray detector development projects described above, the European XFEL has launched separate projects on radiation damage studies, as well as on plasma effect investigations, which occur when large numbers of photons are absorbed in a small sensor volume, creating electron-hole pair concentrations comparable to the doping levels. Finally, a major effort has been initiated in the field of data acquisition and data handling, since the data volumes approach or surpass those common in high energy physics experiments.

## 5 Summary

The source characteristics of the European XFEL under construction in Hamburg, Germany, as well as of the planned experiments, require new and innovative 2-dimensional X-ray detector concepts. The high instantaneous flux available imposes the use of integrating detectors, while at the same time the experiments require single photon sensitivity as well as an extended dynamic range. For the detectors to survive a minimum of three years of operation, they will have to be extremely radiation hard. Three development programs have been initiated by the European XFEL, each attempting to solve the challenges in conceptually different ways. In this paper some of the detector requirements, as dictated by the source and planned experiments, are given and explained, but it is to be understood the many of the parameters will evolve with time, with the experiments getting more defined in detail.

## References

- [1] M. Altarelli et al., *European X-ray Free Electron Laser. Technical Design Report*, ISBN 978-3-935702-17-1 (2006).
- [2] A.M. Kondratenko and E.L. Saldin, *Generation of coherent radiation by a relativistic electron beam in an undulator*, *Sov. Phys. Dokl.* **24** (1979) 986.
- [3] Y.S. Derbenev, A.M. Kondratenko and E.L. Saldin, *On the possibility of using a free electron laser for polarization of electrons in storage rings*, *Nucl. Instrum. Meth.* **193** (1982) 415.
- [4] H.N. Chapman et al., *Femtosecond diffractive imaging with a soft-X-ray free-electron laser*, *Nat. Phys.* **2** (2006) 839.
- [5] R. Neutze, R. Wouts, D. van der Spoel, E. Weckert and J. Hajdu, *Potential for biomolecular imaging with femtosecond X-ray pulses*, *Nature* **406** (2000) 752.
- [6] C. Ponchut, F. Zontone and H. Graafsma, *Experimental comparison of pixel detector arrays and CCD-based systems for X-ray area detection on synchrotron beamlines*, *IEEE Trans. Nucl. Sci.* **52** (2005) 1760.
- [7] M. Campbell et al., *The detection of single electrons by means of a MicrOMEGAs-covered MediPix2 pixel CMOS readout circuit*, *Nucl. Instrum. Meth. A* **540** (2005) 295.
- [8] Ch. Brönnimann et al., *The PILATUS 1M detector*, *J. Synchrotron Rad.* **13** (2006) 120.
- [9] Strüder et al., *Large-Format, High-Speed, X-ray pnCCDs Combined with Electron and Ion Imaging Spectrometers in a Multipurpose Chamber for Experiments at 4th Generation Light Sources*, submitted to *Nucl. Instrum. Meth. A* (2009).

- [10] G. Grübel, G.B. Stephenson, C. Gutt, H. Sinn and Th. Tschentscher, *XPCS at the European X-ray free electron laser facility*, *Nucl. Instrum. Meth. B* **262** (2007) 357.
- [11] J. Als-Nielsen and D. McMorrow, *Elements of modern X-ray physics*, Wiley press, ISBN 0 471 498572 (2001).
- [12] L.J. Koerner, H.T. Philipp, M.S. Hromalik, M.W. Tate and S.M. Gruner, *X-ray tests of a Pixel Array Detector for coherent x-ray imaging at the Linac Coherent Light Source*, *2009 JINST* **4** P03001.
- [13] G.A. Carini et al., *Tests of small X-ray Active Matrix Pixel Sensor prototypes at the National Synchrotron Light Source*, *2009 JINST* **4** P03014.
- [14] X. Shi et al., *Challenges in chip design for the AGIPD detector*, proceedings of the 11<sup>th</sup> ESDD Conference, submitted to *Nucl. Instrum. Meth. A* (2009).
- [15] A. Mozzanica et al., *Characterization of an adaptive gain silicon microstrip readout chip*, proceedings of the 11<sup>th</sup> ESDD Conference, submitted to *Nucl. Instrum. Meth. A* (2009).
- [16] G. Potdevin, U. Trunk and H. Graafsma, *Performance simulation of a detector for 4<sup>th</sup> generation photon sources: the AGIPD*, *Nucl. Instrum. Meth. A* **607** (2009) 51.
- [17] G. Potdevin, U. Trunk and H. Graafsma, *HORUS, an HPAD X-ray detector simulation program*, *2009 JINST* **4** P09010.
- [18] A. Blue, M. French, P. Seller and V. O'Shea, *Edgeless sensor development for the LPD hybrid pixel detector at XFEL*, *Nucl. Instrum. Meth. A* **607** (2009) 55.
- [19] M. Porro et al., *Large format X-ray imager with mega-frame readout capability for XFEL, based on the DEPFET active pixel sensor*, *IEEE Nucl. Sci. Symp. Conf. Rec* (2008) 1578.
- [20] G. Lutz, P. Lechner, M. Porro, L. Strüder and G. De Vita, *DEPFET Sensor with intrinsic Signal Compression Developed for Use at the XFEL Free Electron Laser Radiation Source*, proceedings of the 11<sup>th</sup> ESDD Conference, submitted to *Nucl. Instrum. Meth. A* (2009).
- [21] M. Porro et al., *Spectroscopic performance of the DePMOS detector/amplifier device with respect to different filtering techniques and operating conditions*, *IEEE Trans. Nucl. Sci.* **53** (2006) 401.